



HAL
open science

A novel “ceasefire” model to explain efficient seed transmission of *Xanthomonas citri* pv. *fuscans* to common bean

Armelle Darrasse, Łukasz Pawel Tarkowski, Martial Briand, David Lalanne,
Nicolas W. G. Chen, Matthieu Barret, Jerome Verdier

► To cite this version:

Armelle Darrasse, Łukasz Pawel Tarkowski, Martial Briand, David Lalanne, Nicolas W. G. Chen, et al.. A novel “ceasefire” model to explain efficient seed transmission of *Xanthomonas citri* pv. *fuscans* to common bean. 2025. hal-04338621

HAL Id: hal-04338621

<https://hal.inrae.fr/hal-04338621v1>

Preprint submitted on 14 Jan 2025

HAL is a multi-disciplinary open access archive for the deposit and dissemination of scientific research documents, whether they are published or not. The documents may come from teaching and research institutions in France or abroad, or from public or private research centers.

L'archive ouverte pluridisciplinaire **HAL**, est destinée au dépôt et à la diffusion de documents scientifiques de niveau recherche, publiés ou non, émanant des établissements d'enseignement et de recherche français ou étrangers, des laboratoires publics ou privés.

Copyright

1 **A novel “ceasefire” model to explain efficient seed transmission of *Xanthomonas citri***
2 ***pv. fuscans* to common bean.**

3

4 Armelle Darrasse, Łukasz Paweł Tarkowski, Martial Briand, David Lalanne, Nicolas W.G.
5 Chen, Matthieu Barret, Jerome Verdier

6

7 Univ Angers, Institut Agro, INRAE, IRHS, SFR QUASAV, F-49000 Angers, France

8

9 Author for correspondence: Jerome Verdier

10 jerome.verdier@inrae.fr

11

12 **ORCIDs**

13 Armelle Darrasse: 0000-0002-9334-5862

14 Łukasz Paweł Tarkowski: 0000-0002-5419-6606

15 Nicolas W.G. Chen: 0000-0002-7528-4656

16 Matthieu Barret: 0000-0002-7633-8476

17 Jerome Verdier: 0000-0003-3039-2159

18

19 *Indicate the number of words (Full papers <6,500 words): 6,425*

20 *Indicate the number of figures: 4 figures (all in color), 2 tables, 4 supplementary data*

21

22 **Summary**

23 • Although seed represents an important means of plant pathogen dispersion, the
24 seed-pathogen dialogue remains largely unexplored.

25 • A multi-omic approach (*i.e.* dual RNAseq, plant small RNAs and methylome) was
26 performed at different seed developmental stages of common bean (*Phaseolus*
27 *vulgaris* L.) during asymptomatic colonization by *Xanthomonas citri* *pv. fuscans* (*Xcf*).

28 • In this condition, *Xcf* did not produce disease symptoms, neither affect seed
29 development. Although, an intense molecular dialogue, via important transcriptional
30 changes, was observed at the early seed developmental stages with down-regulation
31 of plant defense signal transduction, via action of plant miR, and upregulation of the
32 bacterial Type 3 Secretion System. At later seed maturation stages, molecular
33 dialogue between host and pathogen was reduced to few transcriptome changes, but
34 marked by changes in DNA methylation of plant defense and germination genes, in
35 response to *Xcf* colonization, potentially acting as defense priming to prepare the
36 host for the post-germination battle. This distinct response of infected seeds during

37 maturation, with a more active role at early stages refutes the widely diffused
38 assumption considering seeds as passive carriers of microbes.

39 • Finally, our data support a novel plant-pathogen interaction model, specific to the
40 seed tissues, which differs from others by the existence of distinct phases during
41 seed-pathogen interaction with seeds first actively interacting with colonizing
42 pathogens, then both belligerents switch to more passive mode at later stages. We
43 contextualized this observed scenario in a novel hypothetical model that we called
44 “ceasefire”, where both the pathogen and the host benefit from temporarily laying
45 down their weapons until the moment of germination.

46

47 **Key words:** Seed, *Xanthomonas*, transmission, dialogue, epigenome, *Phaseolus*
48 *vulgaris*, dual transcriptomics.

49

50 Introduction

51 Legumes provide a sustainable source of proteins for human and livestock diet,
52 moreover their symbiotic nitrogen fixation capacity contributes to soil preservation and
53 reduces the need for chemical fertilizers (Stagnari et al., 2017; Ferreira et al., 2021). An
54 important factor limiting legume utilization is their relatively high yield variability, greatly due
55 to their susceptibility to environmental factors such as biotic and abiotic stresses (Cernay et
56 al., 2015; Martins et al., 2020). While legumes are expected to better perform under
57 changing climatic conditions in relation to other crops thanks to higher biomass accumulation
58 under increased atmospheric CO₂ levels and higher photosynthetic efficiency under
59 increased irradiation levels, other traits are predicted to be negatively affected, such as seed
60 quality and resistance to pathogens (Myers et al., 2014).

61 Pathogens are responsible for 35-70% yield losses on grain legumes (Martins et al.,
62 2020). An important determinant of disease outbreak is pathogen dispersal through infected
63 seeds (Denancé and Grimault, 2022). The mode of transmission of pathogens to the seed
64 can be schematically summarized in three non-exclusive pathways: internal (*via* the host
65 xylem), floral (*via* the pistil) and external as a consequence of contact of the seed with
66 symptomatic fruit tissues or with threshing residues (Maude, 1996). For instance,
67 *Xanthomonas citri* pv. *fuscans* (*Xcf*), causal agent of common bacterial blight of bean (CBB),
68 can use these three pathways for its transmission to common bean seeds (Darsonval et al.,
69 2008; Darrasse et al., 2018). Contaminated seeds can be symptomatic or asymptomatic,
70 and are generally associated with high or moderate bacterial population sizes, respectively,
71 moreover symptomatic seeds often fail to germinate (Darrasse et al. 2018; Chen et al.,
72 2021a) and no viable pathogen control method to counteract bacterial seed infections exists.

73 Decades of research led to a comprehensive overview of the genetic (for review
74 Dodds and Rathjen, 2010; Wirthmueller et al., 2013) and epigenetic (for review Hannan
75 Parker et al., 2022) mechanisms involved in plant-pathogen interactions during vegetative
76 growth. However, the molecular dialogue that takes place between seeds and pathogens
77 was overlooked to date. On the plant side, in the event of an incompatible interaction
78 between *Medicago truncatula* and *X. campestris* pv. *campestris* (*Xcc*), seed transcriptome
79 exhibited an activation of defense response and a repression of seed maturation pathways
80 (Terrasson et al., 2015). From the bacterial side, some specific genetic determinants such as
81 the type 3 secretion system (T3SS, Darsonval et al., 2008) and adhesins (Darsonval et al.,
82 2009) were shown to be involved in the transmission of *Xcf* to common bean seeds.
83 Involvement of the T3SS in seed transmission was also documented for *Acidovorax citrulli* in
84 watermelon (Dutta et al., 2014). However, a global view of bacterial transcriptomic changes
85 occurring during seed transmission is currently missing. This lack of knowledge is partly due
86 to the difficulties of collecting enough bacterial RNA from the seeds. Indeed seed-associated
87 bacterial population sizes are usually very low (from 10 to 1,000 CFU per bean seed;
88 Chesneau et al., 2022) and follow a Poisson distribution, which complicates the sampling of
89 contaminated seeds and prevent molecular analysis of seed-pathogens interactions (Gitaitis
90 and Walcott, 2007).

91 Since knowledge regarding molecular interactions occurring during bacterial seed
92 infections is currently lacking, the objective of this work was to decipher the molecular
93 dialogue between the common bean (*Phaseolus vulgaris* L.) seed and a seed pathogen at
94 several stages of seed development in order to identify major molecular factors involved in
95 seed infection establishment and pathogen transmission to the seedling. A dual RNAseq
96 approach to identify both the host seed and the *Xcf* pathogen transcriptomes was performed
97 at three stages of seed development during seed filling, seed maturation and seed maturity.
98 The technical limitation of low bacterial population within seeds was successfully bypassed
99 using bacterial transcript enrichment. This transcriptomic analysis was complemented by the
100 analysis of small RNAs and DNA methylation changes in infected seeds to reveal the role of
101 these mechanisms in the seed-pathogen interaction, which allowed us to propose a novel
102 model in plant-pathogen interactions specific to seed developmental stage and explaining
103 the efficiency of pathogen seed transmission.

104

105 **Materials and Methods**

106 **Bacterial strain and inoculum preparation**

107 The *Xcf* bacterial strain 7767R (Rif^R, Darrasse et al., 2018) was grown for 24h at
108 28°C in Tryptic Soy Agar at 10% (1.7 g.L⁻¹ tryptone, 0.3 g.L⁻¹ soybean peptone, 0.25 g.L⁻¹

109 glucose, 0.5 g.L⁻¹ NaCl, 0.5 g.L⁻¹ K₂HPO₄ and 15 g.L⁻¹ agar) supplemented with 50 mg.L⁻¹
110 rifamycin. Bacterial cells were suspended in sterile distilled water, calibrated at 10⁸ CFU.mL⁻¹
111 (OD₆₀₀ = 0.1) and adjusted to 10⁶ CFU.mL⁻¹ for spray-inoculation.

112

113 **Plant materials and production of contaminated seeds**

114 Experiments were performed with *Phaseolus vulgaris* L. cv. Flavert, a cultivar
115 susceptible to CBB (Darrasse et al., 2007). Seeds were sown in one liter of Tray substrate
116 (NF U 44–551, Klasmann- Deilmann GmbH, Rippert France). Plants were grown in a
117 controlled growth chamber with 16h of light at 23°C and 8h of dark at 20°C and a relative
118 humidity (RH) of 70%. Plants were watered twice a week during the first three weeks, then
119 with a nutrient solution (N/P/K=15/10/30). Plants were staked and pinched after the third
120 leaf.

121 Plants were spray-inoculated at the flower bud stage (R5, Michael 1994) with either
122 *Xcf* bacterial suspension (10⁶ CFU.mL⁻¹) or water as control. The day prior to inoculation,
123 temperature (day 25°C/night 23°C) and RH (95%) were increased. Inoculation was
124 performed using a two-step protocol. First, small green flower buds were sprayed. Three
125 days later, flower buds at the pollination stage were tagged. Then, a second inoculation was
126 performed at one day after pollination (DAP) when tagged organs turned into open flowers.
127 Then afterward, RH was reduced to 70% to limit pathogen symptom development and seed
128 abortion. Three independent replicates of five plants (*n*=15) were inoculated. Tagged pods
129 were harvested at 24, 35 and 42 DAP. Seeds were collected aseptically from pods to avoid
130 contamination by external bacterial populations (Darsonval et al., 2008).

131

132 **Monitoring of bacterial population sizes**

133 For each sample, *Xcf* population sizes were determined from ten individual seeds and from
134 five pools of three seeds. Seeds were soaked in 0.5 mL of sterile water per seed overnight at
135 4°C under shaking (150 rpm). Then, 50 µL of serial dilutions were plated on 10% TSA.
136 Colonies were monitored five days after incubation at 28°C. The contamination rate of a
137 sample (*p*) was calculated from the analysis of *N* sub-samples according to the formula $p =$
138 $1 - (Y/N)^{1/n}$ (Maury et al., 1985), where *n* is the number of seeds in each group and *Y* the
139 number of healthy groups.

140

141 **Seed physiological analyses**

142 Three sub-samples of ten seeds were used to determine dry weight and water content. Each
143 sub-sample was weighed before and after incubation (3 days) in a 96°C incubator
144 (Memmert).

145

146 **Plant and bacterial RNA extraction and RNA sequencing**

147 Seed samples harvested at 24, 35 and 42 DAP were flash-frozen in liquid nitrogen.
148 Samples were ground in liquid nitrogen using a mechanical grinder (Retsch MM300
149 TissueLyser) during 1 min at 30 Hertz. Total RNAs were extracted using the NucleoSpin[®]
150 RNA Plant and Fungi Kit (Macherey-Nagel, Düren, Germany), according to the
151 manufacturer instructions. RNA quantity and integrity were assessed respectively using a
152 NanoDrop ND-1000 (NanoDrop Technologies, Wilmington, DE, USA) and a 2100
153 Bioanalyzer (Agilent Technologies, Santa Clara, CA, USA). Library constructions and single-
154 end sequencing (SE50, 20M) were outsourced to the Beijing Genomics Institute (BGI,
155 <https://www.bgi.com>) using the Illumina HiSeq 2500 technology. Raw reads are available at
156 GSE226918.

157

158 Using the same seed lots as for plant RNAs, bacterial macerates were collected after
159 soaking contaminated seeds (2 mL per gram of seed) overnight in KPO₄ buffer, (50 mM, pH
160 6.8), supplemented with 20% of blocking agent (RNAlater, ThermoFisher scientific, Carlsbad,
161 CA, United States). After centrifugation (15 min at 15,000 g) and removal of the supernatant,
162 total RNAs were extracted as previously described (Darsonval et al., 2009). Concentration
163 and integrity of RNAs were assessed with Qubit (Invitrogen, Carlsbad, CA, USA) and a 2100
164 Bioanalyzer (Agilent Technologies, Santa Clara, CA, USA), respectively. As total RNA
165 extracted from bacterial macerates corresponded mainly to plant transcripts (not shown), we
166 designed a procedure of bacterial transcript enrichment. Bacterial mRNAs were captured
167 using the SureSelectXT RNA Direct technology (Agilent, Santa Clara, CA, USA). A total of
168 54,548 probes of 120-nts length were designed based on the predicted mRNAs of *Xcf7767R*
169 genome sequence (GCA_900234465; Chen et al., 2018). Quality and quantity of sequencing
170 libraries were evaluated and quantified using Bioanalyzer and KAPA Library Quantification
171 assay (Roche, Basel Switzerland). Paired-end sequencing (2 × 75 bp) was performed with a
172 NextSeq 550 System High OutPut kit (Illumina, San Diego, CA, USA). Raw reads are
173 available at GSE227386.

174 After quality control, high-quality reads were mapped either on *Xcf 7767R*
175 transcriptome (Briand et al., 2021) ([https://bbric-
176 pipelines.toulouse.inra.fr/myGenomeBrowser?browse=1&portalname=Xcf7767Rpb&owner=
177 armelle.darrasse@inrae.fr&key=TwzQ08DA](https://bbric-pipelines.toulouse.inra.fr/myGenomeBrowser?browse=1&portalname=Xcf7767Rpb&owner=armelle.darrasse@inrae.fr&key=TwzQ08DA)) or on *P. vulgaris* transcriptome version 2.1
178 (https://phytozome-next.jgi.doe.gov/info/Pvulgaris_v2_1) using quasi-mapping alignment and
179 quantification methods of Salmon algorithm v.1.2 (Patro et al., 2017). RNA-Seq data were
180 normalized as transcripts per million (TPM). Differentially expressed genes (DEGs) were
181 determined using DESeq2 v1.22.2 (Love et al., 2014), using an adjusted p-value <5%. *Xcf*
182 DEGs were analyzed between sampling dates. *P. vulgaris* DEGs were obtained by

183 comparing *Xcf*- versus H₂O-inoculated seeds at each developmental stage. Gene
184 annotations were provided with the *P. vulgaris* version 2.1 genome and Mapman functional
185 categories v.4 were determined using Mercator tool from the predicted protein sequences
186 (Schwacke et al., 2019). Over representation analyses of MapMan or COG terms were
187 performed, respectively for plant and bacteria DEGs, using Clusterprofiler (Yu et al., 2012)
188 package in R by applying an adjusted p -value cut-off <0.05 obtained after the Bonferroni-
189 Hochberg procedure.

190 Differentially expressed genes during seed germination were identified using the data
191 generated by Narsai et al. (2017) available in the SRA database (accession GSE94457).
192 Raw reads were downloaded and mapped against the Arabidopsis transcriptome using
193 Salmon algorithm and DEGs during germination kinetic were determined using ImpulseDE2
194 algorithm (Fischer et al., 2018) following an adjusted p -value $<1\%$.

195 To determine genes involved in post-germination defense, we inoculated healthy
196 seeds with 10^7 of *Xcf* CFU.mL⁻¹ or H₂O during 25 min under gentle agitation followed by 3
197 min of vacuum infiltration before seed drying at 25°C. Inoculated dried seeds displaying
198 between 10^4 and 10^5 CFU.seed⁻¹ of *Xcf* were used for germination assay on Whatman paper
199 in 16h-light growth chamber at 25°C. *Xcf*- and H₂O-inoculated seeds were collected at 3 and
200 7 Days After Imbibition (DAI) and dissected as separated cotyledons and radicles for real-
201 time qRT-PCR experiments. RNA were extracted at different germination timepoints and in
202 different tissues using the NucleoSpin® RNA Plant and Fungi Kit (Macherey-Nagel, Dußen,
203 Germany) as described above but including a DNase treatment (Macherey-Nagel, rDNase
204 set, Dußen, Germany). RNA were quantified using a using a NanoDrop ND-1000
205 (NanoDrop Technologies, Wilmington, DE, USA) and cDNA was synthesized from 1 µg of
206 total RNA using the Reverse Transcription system (iScript™ cDNA synthesis kit, Bio-Rad).
207 Quantitative Real time PCR was performed using Sybr Green Master Mix (SYBR Green
208 master mix, Bio-Rad) on a CFX96 real-time detection system (Bio-Rad Laboratories). *EF1*
209 and *UBI* genes were used as housekeeping genes as described in Darrasse et al. (2010).
210 Primers used for Real-time PCR are listed in Supplementary Table S4.

211

212 **small RNA extraction and analysis (sRNA-seq)**

213 Using the same frozen powders obtained from *Xcf*- and H₂O-inoculated seeds from
214 24 DAP and 42 DAP, we extracted small RNA using the NucleoSpin® miRNA Kit
215 (Macherey-Nagel, Dußen, Germany), according to the manufacturer's instructions. Small
216 RNA enrichment was validated using Bioanalyzer small RNA analysis. Small RNAs were
217 sequenced using DNBseq sequencing technology (SE50 40M, BGI) and Unique Sequence
218 identifiers (UMI) to correctly quantify unique reads. Reads of 20 to 24 nucleotides were

219 extracted and mapped on the reference mature miRNA database available in miRBase
220 version 22 (Kozomara et al., 2019) using bowtie (Langmead et al., 2009) and quantified
221 using SAMtools (Li et al., 2009). Differentially expressed small RNA between *Xcf*-inoculated
222 versus H₂O-inoculated seeds at 24 and 42 DAP were determined using DESeq2 following a
223 *p*-value threshold < 5% from the SARTools R package (Varet et al., 2016). Known and
224 putative novel small RNAs were mapped to the *P. vulgaris* genome sequence using
225 ShortStack4 algorithm (Johnson et al., 2016) and displayed in the dedicated Jbrowse
226 https://iris.angers.inrae.fr/pvulgaris_v2 in the 'small RNA tracks' section. Transcripts
227 potentially targeted by miRNAs were predicted via analyzing complementary matching
228 between sRNA and target and evaluating target site accessibility using psRNATarget tool
229 (Dai and Zhao, 2011; Dai et al., 2018) and a threshold of expectation below 5 was set to
230 consider transcripts as putative miRNA targets. Raw reads are publicly available at
231 GSE226920.

232

233 **Plant DNA extraction and Bisulfite sequencing experiments (BS-seq)**

234 From the same frozen seed powders used for RNA extractions, we performed DNA
235 extraction, on the three biological replicates of *Xcf*- and H₂O-inoculated seeds at 42 DAP,
236 using the NucleoSpin® DNA Food Kit (Macherey-Nagel, Düren, Germany), according to
237 the manufacturer's instructions. DNA samples were sent to the BGI Genomics (Hong Kong)
238 for bisulfite treatment using a ZYMO EZ DNA Methylation™ Gold kit, library construction and
239 paired-end sequencing using BGISEQ-500 sequencing technology (PE100 45M). FastQC
240 was used to check sequencing quality and clean reads were mapped to the *P. vulgaris*
241 genome version 2.1 using Bismark software (Krueger and Andrews, 2011). After mapping,
242 deduplication of sequences and quantification of cytosine methylation were performed using
243 Bismark_deduplicate and Bismark_methylation_extractor. Each context of methylation was
244 considered independently: CG, CHG, or CHH and corresponding bigwig files were
245 generated using bismark_to_bigwig python script and displayed in the dedicated Jbrowse:
246 https://iris.angers.inrae.fr/pvulgaris_v2. Putative differentially methylated regions (DMRs)
247 were identified in each independent methylation context using DMRCaller algorithm
248 available in R (Catoni et al., 2018). Raw reads are publicly available at
249 <https://www.ncbi.nlm.nih.gov/geo/query/acc.cgi?acc=GSE226919>.

250

251 **Results**

252 ***Seed transmission of moderate Xcf population sizes does not impact seed***
253 ***development***

254 Seed transmission of *Xcf* 7767R was investigated following spray-inoculation of *P.*
255 *vulgaris* L. cv Flavert. Three stages of seed development were targeted: (i) 24 DAP (seed
256 filling), (ii) 35 DAP (seed maturation) and 42 DAP (seed maturity). Seed water content (Fig.
257 1A) and dry seed weight (Fig. 1B) were not significantly impacted by *Xcf*-inoculation. As
258 described in Darsonval et al. (2008), we used 10^6 CFU.mL⁻¹ for *Xcf* spray-inoculation at
259 flowering time to allow seed bacterial transmission without apparition of symptoms during
260 seed development. Otherwise, higher concentration could generate symptomatic seed
261 bacterial transmission leading to defect in germination of infected seeds. Following this mild
262 treatment, about 80% of seeds were contaminated with *Xcf* with an average population size
263 of 10^5 CFU.g⁻¹ of seeds at 24 DAP (Fig. 1C). Over the course of seed development, the
264 frequency of detection of *Xcf* decreased from 80% to 50%. This was accompanied by a
265 significant decrease in *Xcf* population size from 35 to 42 DAP, down to an average of 10^3
266 CFU.g⁻¹ of seeds at maturity (Fig. 1C).

267 ***Changes in the Xcf bacterial transcriptome during seed development***

268 To explore the genetic determinants involved in *Xcf* seed transmission, dual (host
269 and pathogen) transcriptome sequencing was performed at 24, 35 and 42 DAP. An essential
270 step to obtain sufficient bacterial transcript data was to enrich RNA-Seq libraries for *Xcf*
271 transcripts using 54,656 capture-probes. Among a total of 27.7 to 61.3 M sequenced reads
272 that were obtained for each sample, 4.7 to 55.1 M mapped on the predicted transcriptome of
273 *Xcf* strain 7767R (Supplementary Table S1). A total of 4,372 mRNA were detected in at least
274 one sample (count ≥ 10), which corresponded to >96% of the 4,537 predicted mRNA, thus
275 validating our *Xcf* transcriptome enrichment strategy. Extensive changes in *Xcf*
276 transcriptome were observed between seed filling (24 DAP) and the two other seed
277 maturation stages (35 and 42 DAP). Indeed, 865 and 1,674 DEGs were detected between
278 24 and 35 DAP and 24 and 42 DAP, respectively, (Fig. 2A). On the other hand, only 17
279 DEGs were detected between 35 and 42 DAP, indicating that transcriptomic levels stabilized
280 between seed maturation and maturity stages. In line with this result, over-representation
281 analyses of COG terms associated to bacterial DEGs were performed and revealed that
282 intracellular trafficking and secretion terms were enriched at 24 DAP and post-translational
283 modification at 35 and 42 DAP (Fig. 2B). The other enriched categories were translation and
284 repair/ repair, both enriched at 42 DAP, and extracellular structure and cell motility, both
285 enriched at 24 DAP (Fig. 2B).

286 A focus on the COG related to secretion processes revealed that all T3SS encoding
287 genes and several *xps* genes involved in the T2SS were up-regulated at the seed filling
288 stage, but not later during seed maturation (Supplementary Table S1). This was consistent

289 with the observed up-regulation of the master regulator *hrpG* that is known to control many
290 genes involved in the interaction with the host plant (Teper et al., 2021) such as the T3SS
291 transcriptional activator *hrpX* and cognate effectors (T3Es) but also the *xps* genes involved
292 in the secretion of cell wall degrading enzymes (Szczeny et al., 2010). In line with this
293 result, 26/41 (63.4%) of T3E-encoding genes and several genes encoding pectin lyase (1),
294 pectate lyases (2), glycoside hydrolases (34) and proteases (40) were only up-regulated at
295 early stage (Supplementary Table S1). Together, these results suggested that bacteria were
296 actively interacting with the host plant only at early seed maturation stages, but not later.

297 ***Transcriptomic analysis of bean seeds in response to pathogen colonization***

298 Changes in *P. vulgaris* transcriptome were assessed using the same seed lots as for
299 the *Xcf* transcriptome analyses described above. All results from this RNA-Seq analysis are
300 displayed in the dedicated Jbrowse (https://iris.angers.inrae.fr/pvulgaris_v2) and in
301 Supplementary Table S1. Similar to what was observed in *Xcf* transcriptome changes, RNA-
302 Seq analysis revealed that the plant response to the bacteria was higher at early than later
303 stages of seed maturation, with 1,826 DEGs at 24 DAP, 1,351 at 35 DAP and only 105 at 42
304 DAP (Fig. 2C). Only 137 DEGs (7.5% of 24 DAP DEGs) were shared between 24 and 35
305 DAP, indicating that the plant's response was different between these stages, ending up with
306 almost no response in mature seeds. Only one DEG, encoding a CHAPERONE PROTEIN
307 DNAJ-LIKE PROTEIN, was found to be in common between all the three stages
308 (*Phvul.001G262000*) and could reflect a cellular stress in seeds inoculated with *Xcf*. This
309 low overlap in DEGs across different seed developmental stages was also reflected at the
310 level of functional category enrichments, which were different between 24, 35 and 42 DAP
311 (Fig. 2D). The 24 DAP timepoint displayed the most complex response, with six up-regulated
312 and nine down-regulated Mapman functional categories detected through functional
313 enrichment analysis of DEGs. Some categories had well characterized roles in the plant-
314 microbe molecular dialogue, such as Leucine Rich Repeat protein kinases (LRRs), which
315 were up-regulated in *Xcf*-inoculated seeds (*i.e.* up-regulation of 15 annotated LRR related
316 proteins), whereas the Mitogen-Activated Protein Kinases (MAPKs) and transcription factors
317 (TF) of the bZIP, TIFY and AP2/ERF classes were down-regulated. At 24 DAP, in parallel to
318 the down-regulation of MAPKs known to be involved in defense signal transduction such as
319 MAPKKK3, MAPK3 or MAPK4, we also identified down-regulation of defense related genes
320 such as two encoding thaumatin pathogenesis-related (PR) proteins, five *JAZ* and one *JAR*
321 genes involved in the jasmonic acid pathway, but also *PAD4*, a central regulator of the
322 salicylic acid pathway (Supplementary Table S1). At 35 DAP, functional ontology enrichment
323 detected four up-regulated categories related to peptidase/protease activities and transfer of

324 carbon skeletons. At 42 DAP, only two up-regulated categories (chromatin regulation and
325 calcium-permeable channel) were detected.

326 ***Small RNAs associated with Xcf seed colonization***

327 To further characterize the molecular dialogue between the colonized seeds and *Xcf*
328 and the changes in plant transcript expression we focused our analysis on small RNA
329 changes between colonized and healthy seeds at two contrasted stages, at 24 DAP to
330 decipher if transcriptome changes due to plant response to pathogen could be mediated by
331 small RNAs and at 42 DAP to reveal if specific small RNA could be stored at seed maturity
332 to mediate defense response at post-germinative stage. Following sequencing and mapping
333 against the mature miRNA database (miRBase release 22), we observed a total of 255 and
334 112 mature miRNAs differentially expressed ($p < 0.05$) between *Xcf*-colonized and healthy
335 seeds at 24 and 42 DAP, respectively. At 24 DAP, mature miRNA up-regulated in *Xcf*-
336 colonized seeds belonged to six miRNA families (miR162, miR172, miR396, miR482,
337 miR6478 and miR8175), while four miRNA families showed down-regulation (let7, miR21,
338 miR2111 and miR482) (Supplementary Table S2, Table 1). Similarly, at 42 DAP, we
339 observed up-regulation of only one miRNA family (miR31) and down-regulation of two
340 miRNA families (miR164 and miR451) (Supplementary Table S2, table 1). These data
341 further confirmed that the molecular dialogue was more intense at early stages compared to
342 later stages. Moreover, several miRNA families differentially regulated in *Xcf*-inoculated
343 seeds were known to be involved in plant defense response such as miR482 (Shivaprasad
344 et al., 2012), miR396 (Soto-Suárez et al., 2017) and miR172 (Holt et al., 2015). Known and
345 unknown identified small RNAs were mapped to the genome using ShortStack version 4 and
346 are available in the dedicated *P. vulgaris* Jbrowse (https://iris.angers.inrae.fr/pvulgaris_v2).

347 To reveal the potential response mediated by these miRNAs, we identified putative
348 transcript targets using (i) psRNATarget predictive tool (Dai et al. 2018) combined with (ii)
349 our generated transcriptomic data at these two stages (Supplementary Table S2). To clarify,
350 a transcript was considered as putative miRNA target if (i) its expectation (E) score from
351 PsRNATarget was below 5 and if (ii) its expression was down-regulated when miRNA was
352 up-regulated or inversely. Following these criteria, we identified between one to 11 putative
353 miRNA target transcripts depending on miRNA families (Table 1). Among miRNAs up-
354 regulated at 24 DAP in *Xcf*-inoculated, there were target transcripts related to defense such
355 as miR8175 that could down-regulate key defense genes such as *PAD4-LIKE* involved in the
356 defense pathway mediated by salicylic acid or more generic ones potentially involved in
357 defense signaling such as a calcium-dependent-lipid-binding domain gene (CalB) or
358 phospholipase A1 (Table 1). At the opposite, in the *Xcf*-inoculated seeds, we observed

359 down-regulation of miRNA families such as let7, miR21, miR2111 and miR482 that
360 potentially enhanced expression of developmental/growth genes such as TOR-LIKE,
361 MED15, MED13, NOC1/SWA2. At 42 DAP, only three miR families, miR31, miR451 and
362 miR164, showed significant expression changes between *Xcf*-infected and healthy seeds.
363 An unique putative transcript target was identified associated with miR451, which encodes a
364 UBP26-LIKE protein potentially involved in the heterochromatin silencing at the end of the
365 seed maturation (Luo et al., 2008). In conclusion, these results suggested that miRNA did
366 mediate seed growth by silencing defense response at 24 DAP during early seed
367 development. On the other hand at maturity, even if miR164 up-regulation was already
368 shown to be involved in plant defense against fungi in cotton (*Gossypium hirsutum*) and
369 *Populus tomentosa* (Hu et al., 2020; Chen et al., 2021b), in our susceptible host this miR
370 was down-regulated at 42 DAP, which did not support the hypothesis that specific miRNA
371 were accumulated in *Xcf*-inoculated seeds to prepare plant defense during germination.
372 Interestingly, at 24 and 42 DAP, we observed that plant miRNA could support seed defense
373 silencing probably due to the bacteria infection arsenal such as its T3Es activated early
374 during seed development.

375 ***Seed methylome dynamics associated with Xanthomonas seed colonization***

376 To better understand the plant defense response and the impact of the bacterial
377 colonization during seed development, we analyzed the changes in the seed methylomes of
378 healthy and *Xcf*-colonized bean seeds at seed maturity (42 DAP). Indeed, DNA methylation
379 was already described as a relevant mechanism in defense priming and plant immunity (for
380 review see Deleris et al., 2016; Espinas et al., 2016). By focusing on the mature stage, we
381 intended to capture the cumulative impact on DNA methylation of the bacterial colonization
382 throughout seed development. The comparison of *Xcf*-colonized versus healthy seeds
383 samples revealed 954 Differentially Methylated Regions (DMRs), of which 61.95% were
384 hypomethylated (loss of methylation due to bacterial colonization) and 38.05%
385 hypermethylated (gain of methylation due to bacterial colonization) (Supplementary Table
386 S3). Not surprisingly, DMRs were predominantly localized on sequences containing
387 transposable elements or repeats (74.1% of total DMRs), while 7.9% and 4.5% were located
388 within gene and promoter sequences, respectively (Fig. 3A). Regarding the methylation
389 context, we mainly observed DMRs in the CHH (*i.e.* 481 DMRs) and CHG (*i.e.* 394 DMRs)
390 contexts, while only 79 were related to the CG context. The complete list of the differentially
391 methylated genes can be found in Supplementary Table S3 and in the dedicated Jbrowse
392 (https://iris.angers.inrae.fr/pvulgaris_v2).

393 We identified a total of 102 DMRs located within either coding (n=66) or promoter
394 regions (n=36) of annotated genes, affecting 99 unique genes. Among coding sequences,
395 33 genes resulted in hypomethylation and 33 hypermethylation, while among promoter
396 regions 27 genes were hypomethylated and 9 hypermethylated (Fig. 3B). To understand the
397 role of genes differentially methylated in promoter and coding sequences at seed maturity,
398 we compared with their changes in expression and did not observe any overlap with the
399 DEGs between *Xcf*-colonized and non-colonized mature seeds, suggesting that differentially
400 methylated regions did not regulate gene expression during seed development. To
401 understand the potential role of these DMRs in the host-pathogen interaction, we looked at
402 genes involved both in the germination and defense processes. First, from the dataset
403 generated from Narsai et al. (2017) during ten early stages of *A. thaliana* seed germination,
404 we identified 21,015 genes showing a differential expression (adjusted *p*value <1% using
405 ImpulseDE2) during germination process, therefore potentially involved in germination. By
406 mapping *P. vulgaris* transcripts on Arabidopsis transcripts, we identified potential
407 homologous transcripts in these two species and revealed a statistically significant
408 enrichment (Fig. 3B, Fisher's Exact test *p*-value < 2.2e-16) of *P. vulgaris* genes displaying
409 DMRs following pathogen colonization with those differentially expressed during
410 germination. Indeed, out of the 90 homologous genes identified in *A. thaliana* and displaying
411 DMR, 78 were genes differentially expressed during germination (Fig. 3C). Second, by
412 analyzing the list of 99 unique genes displaying changes in methylation levels following
413 bacterial colonization, we compiled a list of genes with putative roles in defense. We
414 identified 17 genes, 10 hypomethylated and 7 hypermethylated following bacterial infection
415 (Table 2). As example, we observed five LRR-related protein kinases, two PR proteins, and
416 some genes identified as involved in immune response such as *PUB13-LIKE*, *CES11-LIKE*
417 or *WRKY72* (complete list in Supplementary Table S3). As it is known that changes in the
418 methylation state of transposable regions can also spread to adjacent regions and regulate
419 nearby gene expression (Ahmed et al., 2011), we extended our search to coding sequences
420 that are 5kb nearby DMRs located in transposable regions. This analysis detected additional
421 280 genes potentially associated with DMRs located in transposable regions (61.4% with
422 hypomethylated regions and 38.6% with hypermethylated regions). Among these genes, we
423 observed a subgroup coding for disease resistance proteins, with 5 additional putative TIR-
424 NB-LRR proteins (*Phvul.004G105600*, *Phvul.004G100300*, *Phvul.010G026400*,
425 *Phvul.010G027900*, *Phvul.010G028000*), 3 putative NB-ARC proteins (*Phvul.002G130300*,
426 *Phvul.002G130400*, *Phvul.004G076100*) and 4 putative LRR kinases (*Phvul.008G164500*,
427 *Phvul.008G164600*, *Phvul.005G162100*, *Phvul.005G162000*) (Table 2, Supplementary
428 Table S3 and in the dedicated Jbrowse). In total, we listed 17 DMRs nearby genes
429 associated with defense processes (Table 2). A comparison between these two lists

430 revealed that 5 genes encoding three *LRR related proteins* (*Phvul.008G164600*,
431 *Phvul.005G162000* and *Phvul.005G163000*), one *TIR NBS LRR protein*
432 (*Phvul.010G026400*) and *WRKY72 TF* (*Phvul.003G068700*), displayed DMRs both within
433 their gene sequences and in transposable elements located in proximal genomic regions. To
434 define if these DMRs present in defense genes could be associated to a mechanism of
435 defense priming induced by the presence of the pathogen during seed development, we
436 selected the most differentially methylated, the *WRKY72* gene, and validated its implication
437 in *Xcf* response during germination. By qRT-PCR, we analyzed the expression profile of
438 *WRKY72* during germination in healthy seeds that germinated in presence of water versus
439 *Xcf*. We clearly observed an over-expression of *WRKY72* at 7 days after imbibition in radicle
440 of germinated seeds in presence of *Xcf*, showing the role of this gene in the defense
441 response to *Xcf* infection during germination (Fig. 3D).

442 Together, these results suggested that DMRs due to the presence of *Xcf* were mainly
443 located in genes that could serve during the germination process and/or to the plant immune
444 response to *Xcf*. In other word, pathogen-specific DNA methylations occurring during seed
445 development could serve as defense priming to regulate gene expressions during the
446 germination process, including a resumption of the molecular dialogue with the pathogen.

447

448 Discussion

449 Seeds are essential components of plants fitness and represent an important means
450 of pathogen dispersion. To date, seed-pathogen interactions have been understudied at the
451 molecular level, with, to our knowledge, only one plant-orientated study describing the
452 transcriptomic response of *Medicago truncatula* seeds to bacterial pathogens of the
453 Xanthomonadaceae family (Terrasson et al., 2015). We thus attempted to mitigate this
454 knowledge gap by describing the molecular dialogue between common bean seeds and *Xcf*
455 in conditions that seed bacterial transmission was asymptomatic. A first central result
456 regarding this interaction is that *Xcf* was able to colonize seeds without major impact on
457 seed physiology parameters, which was reflected by similar dry weights and water contents
458 in healthy- and infected-seeds (Fig. 1). Consequently, we could not observe any obvious
459 morphological changes in *Xcf*-colonized seeds compared to mock treated samples. Such
460 findings indicate that asymptomatic *Xcf* colonization does not impact seed development or
461 alter seed growth. This is consistent with previous report in *M. truncatula* during compatible
462 interaction with *X. alfalfae* subsp. *alfalfae*, while incompatible interaction with *X. campestris*

463 *pv. campestris* resulted in developmental defects alongside a strong activation of defense
464 pathways (Terrasson et al., 2015).

465 To look into molecular dialogue, transcriptomic changes were assessed using dual
466 RNAseq, which implies that we profiled both bacterial and plant transcripts during seed
467 development generating the first dual transcriptomic analysis of a seed-pathogen interaction
468 ever made. Profiling of bacterial transcripts represented the main challenge we faced due to
469 the low concentration of bacterial cells within seeds. In this study, we successfully achieved
470 this technological breakthrough by an enrichment step of bacterial transcripts using an RNA
471 capture technology provided by Agilent. Our study revealed that *Xcf* and common bean
472 seeds establish an intense molecular dialogue at the early stages of seed development that
473 appears to become less intense as seed maturity approaches (Fig. 2).

474 On the pathogen side, the up-regulation of the T3SS genes and cognate effectors
475 observed in the early stages in comparison with 42 DAP suggests they could play a role in
476 the host defense silencing during the early step of seed colonization (Buttner, 2016). Indeed
477 xanthomonads T3SS and T3Es are known to play a crucial role in suppressing plant innate
478 immunity and modulate plant pathways for the benefits of the bacteria (Büttner, 2016). This
479 further supports previous studies on the importance of T3SS in common bean seeds
480 colonization by *Xcf* (Darsonval et al., 2008). Interestingly, down-regulated categories at early
481 stages include basic biological processes such as translation, protein turnover and DNA
482 replication. This might suggest that *Xcf* multiplication is hampered, consistently with the
483 observation that number of *Xcf* cells in seeds does not increase significantly throughout seed
484 developmental stages (Fig. 1C). Fewer functional categories were enriched at 35 DAP (Fig.
485 2D). The up-regulated ones (4 out of 5) included peptidases, glycosylases and methyl
486 transferases. Such functions can be associated with both suppression of defense
487 (peptidases, Figaj et al., 2019) and cell wall remodeling, which could help bacterial
488 colonization of seed tissues, with no detectable impact on the seed physiology and
489 morphology, although more subtle microscopical effects cannot be excluded (Fig. 1).

490 On the host side, we also observed intense gene expression changes at early seed
491 developmental stage (24 DAP) in comparison to later ones, concomitantly with the intense
492 bacterial secretion activity. We observed an enrichment of up-regulated Leucine Rich
493 Repeat (LRR) protein kinases (2 categories out of 6, LRR class VIII and class Xb), which are
494 known to have prominent roles in microbe perception and defense activation in non-seed
495 tissues (Chakraborty et al., 2019), suggesting that the host may be able to recognize the
496 pathogen. On the other hand, RNA-Seq data highlighted a down-regulation of gene
497 categories with well characterized roles in the transduction of defense signaling pathways,
498 including Mitogen-Activated Protein Kinases (MAPKs such as MAPKKK3, MAPK3 or
499 MAPK4) and transcription factors of the bZIP (basic leucine ZIPper), TIFY, and AP2/ERF

500 (APETALA 2/ Ethylene Responsive Factor) families (Bethke et al., 2009; Bai et al., 2011;
501 Tintor et al., 2013; Noman et al., 2017). In line with this, we observed down-regulation of
502 transcription factor families known to have wider functions in plant stress signaling, such as
503 the TUB or TLP (TUBBY-Like Proteins) and the HSF (Heat Shock Transcription factor), as
504 well as genes encoding PR proteins, including *JAZ* and *JAR* genes involved in the jasmonic
505 acid pathway, and *PAD4* involved in the salicylic acid pathway. Such data suggest that even
506 the transduction components of the defense pathway are inhibited, potentially due to the
507 bacterial T3E, ultimately avoiding a defense response.

508 Similar to transcriptomic data, changes in expression of small RNA at 24 DAP and 42
509 DAP were consistent with silencing of downstream defense gene response. Indeed, analysis
510 of the differentially expressed miRNA at 24 DAP and their putative target genes suggest a
511 growth/defense trade-off mechanism in favor of growth in *Xcf*-inoculated seeds, with down-
512 regulation of defense-associated transcripts (e.g. putative ortholog of *PAD4*
513 (*Phvul002G274500*, Phyto Alexin Deficient 4, involved in salicylic acid signaling in *A.*
514 *thaliana* (Pruitt et al., 2021)), a pepsin-type protease (*Phvul001G229200*) and up-regulation
515 of development-associated transcripts (e.g. TOR-LIKE (*Phvul011G050300*) and
516 *MED15* (*Phvul010G157900*, MEDIATOR 15, required for correct embryogenesis in *A.*
517 *thaliana* (Kim et al., 2016)). Interestingly, a heat shock protein (*HSP70*, *Phvul003G154800*)
518 was detected as down-regulated genes at 24 DAP in *Xcf*-inoculated seeds and potential
519 target of miR396, which complete the observed downregulation of HSF and smallHSP from
520 our infected host transcriptome data (Fig. 2D). Recently it was showed that heat shock
521 proteins are the most represented family among the down-regulated DEGs in leaf in a
522 resistant common bean genotype towards common bacterial blight (caused by *Xcf* and
523 *Xanthomonas phaseoli* pv. *phaseoli*) in comparison to a susceptible one (Foucher et al.,
524 2020). On the other hand, data obtained at 42 DAP revealed only down-regulation of one
525 miRNA family miR451, potentially regulating the up-regulation of its predicted target gene
526 (*Phvul009G100000*) (Table 1). Its *A. thaliana* homolog (AT3G49600.1) deubiquitinates the
527 histone H2B and is required for heterochromatin silencing during seed development (Luo et
528 al., 2008). It is worth noting that chromatin reorganization processes due to histone
529 modifications are among the categories enriched at 42 DAP (Fig. 2D), therefore suggesting
530 that epigenetic regulation is a relevant component of the seed-pathogen molecular dialogue
531 at this stage, potentially acting as priming for post-germination phase. Globally, the
532 transcriptomic response of the susceptible host plant suggests that developing seeds are
533 able to perceive the pathogen, and that defense responses might be largely inhibited by the
534 bacterial T3SS arsenal. Consistent with suppression of the plant defense, up-regulation of
535 photosynthesis and down-regulation of cell wall organization enzymes (Fig.2D) were also
536 previously observed in leaves of susceptible common bean plants upon infection (Foucher et

537 al., 2020). On the other hand, down-regulation of HSP and HSF, and AP2/ERF transcription
538 factors (Fig.2D) were the hallmark of resistant plants. This suggests that a balance between
539 susceptibility and resistance exist in *Xcf*-infected seeds, which could explain why, despite
540 active bacterial colonization, the seeds were asymptomatic and presented no obvious
541 physiological impact.

542

543 In this study, we also revealed that DNA methylation changes in *Xcf*-inoculated seed
544 may also act as defense priming for post-germination phase. Indeed, the seed host
545 methylome analysis at 42 DAP revealed significant changes in methylation status in 826
546 different genomic regions, affecting a total of 99 different genes, which did not display any
547 change in gene expression during seed maturation. Of these, 17 can be associated to
548 defense processes in a relatively straightforward manner (Table 2). As hypomethylation of
549 defense genes has been widely associated with increased resistance to biotic stress (Dowen
550 et al., 2012; Annacondia et al., 2021), the hypomethylated genes of this list (10 out of 17)
551 can be considered as candidates for epigenetic-dependent defense priming. The concept of
552 defense priming postulates that plants conserve the memory of previous encounters with
553 pathogens by preparing their defense networks to respond more rapidly and strongly to a
554 future aggression (Martinez-Medina et al., 2016). Enhanced chromatin access to defense
555 genes through hypomethylation is one of the best characterized mechanisms in this sense
556 (Hannan Parker et al., 2022). Furthermore, epigenetic defense priming can be transmitted to
557 the next generations (Slaughter et al., 2012). This would be consistent with a scenario where
558 *Xcf* colonization does not directly induce defense gene activation in common bean seeds,
559 but rather triggers a primed state that prepare defense networks for the moment when the
560 pathogen will again become virulent (after germination). Hypomethylation of transposable
561 elements is another well-characterized mechanism of epigenetic regulation of plant
562 defenses, as it can lead to the euchromatisation of wide genomic regions, both proximal and
563 distal (López Sánchez et al., 2016; Halter et al., 2021). The five defense genes present in
564 Table 2 are thus likely to be good candidates for relevant roles in bean resistance against
565 *Xcf*. They include three genes affected by hypomethylation (*Phvul.008G164600*,
566 *Phvul.005G163000*, *Phvul.010G026400*), namely two putative LRR kinase receptors and
567 one effector receptor, all uncharacterized. The other two genes affected by hypermethylation
568 are another uncharacterized LRR kinase receptor (*Phvul.005G162000*) and the putative
569 bean homolog of WRKY72 (*Phvul.003G068700*). This transcription factor has the highest
570 methylation gain among all the genes detected (fold change of +4,3), suggesting that its
571 methylation status might be important in response to *Xcf* infection. Indeed, the role of
572 WRKY72 orthologs is contradictory in different species. A positive role on defense
573 responses was showed in *A. thaliana* and tomato (*Solanum lycopersicum*) against

574 oomycetes and bacteria, respectively (Bhattarai et al., 2010), but regarding the interaction
575 between rice (*Oryza sativa*) and *Xanthomonas oryzae* pv. *Oryzae*, it was showed to
576 negatively regulate rice defense responses by repressing jasmonate biosynthetic genes
577 (Hou et al., 2019). In our study, we validated its role as *Xcf*-response genes during
578 germination by highlighting its over-expression at 7 DAI in radicles of germinated seeds in
579 presence of *Xcf*. Another consideration regarding our methylome data is the high overlap
580 between DMRs-containing genes and germination-DEGs (Fig. 3B). This suggests that the
581 DMR-containing genes following bacterial infection detected in this study may serve during
582 the germination process through a defense priming mechanism. More investigation will be
583 required to define if these methylation changes will have positive or negative impacts on
584 defense- and/or germination-related gene expressions and will require extensive
585 transcriptomic analyses.

586

587 All together, these results indicate that the molecular mechanisms involved in the
588 pathogen-seed dialogue change radically across the developmental stages for both the host
589 and the pathogen side, potentially suggesting the existence of distinct phases in the
590 considered seed-pathogen interaction. It would be interesting to explore whether such
591 pattern takes place in other seed-pathogen interactions. By summing our physiological and
592 molecular observations, with the previous findings of Terrasson et al. (2015), we can
593 propose a model where the recognition of a host-specific pathogen at the early stages of
594 seed development fails to trigger seed defense activation, as if the presence of the pathogen
595 was “accepted” by the host. Even if we cannot define whether this suppression is caused by
596 the pathogen or by the host, two *Xanthomonas* studies would support the role of bacterial
597 T3SS in host defense silencing. Darsonval et al. (2008) showed the requirement of T3E for a
598 successful seed colonization in the *Xanthomonas fuscans* sp. *fuscans*-bean seed interaction
599 and Terrasson et al. (2015) showed that *Xcf* was able to silence some defense genes in a
600 compatible interaction, but not in an incompatible one. In any case, the result is a situation
601 where the seed develops normally without any obvious fitness costs associated to an
602 eventual defense activation, while the host-specific pathogen displays a non-aggressive
603 behavior throughout all the seed development and limits its proliferation (Fig. 4). Such
604 “ceasefire” scenario might be advantageous for both parts: the seed is able to reach
605 maturity, which would potentially be beneficial for the pathogen as well by allowing it to infect
606 the future germinated seedling, therefore giving it access to nourishment and facilitating its
607 dispersal. On the other hand, data at 42 DAP suggest a relevant role for epigenetic
608 modifications in the host. It is tempting to speculate that such modifications contribute to
609 prepare the host to face a novel pathogen assault after germination (Fig. 4). Detailed
610 analysis of the transcriptome and epigenome of the bean-*Xcf* interaction during the

611 germination process would be a promising future research direction in this sense. Recent
612 data from the compatible interaction *Alternaria brassicicola*-*A. thaliana*, used as seed
613 transmission model, showed that host defense pathways are subjected to drastic changes
614 during the germination process (Ortega-Cuadros et al., 2022). It would be interesting to
615 explore whether such rearrangements take place in other compatible interactions such as
616 *Xcf*-bean and if a link with epigenetic modifications exists.

617

618 To summarize, the present study adds novel elements to the current knowledge gap
619 of seed-pathogen interactions. The dual transcriptomic analysis allowed for the first time to
620 describe the molecular dialogue from both host and pathogen sides, while methylome and
621 sRNAs profiling added further indications on the potential regulatory mechanisms and the
622 genes involved. A dedicated Jbrowse containing all these generated data will serve as
623 baseline tool for the scientific communities and will be enriched by future related studies. An
624 important general conclusion that we can draw is that seeds have primarily an active role in
625 this interaction at early seed maturation stage, contrary to the widely diffused assumption
626 considering seeds as passive carriers of microbes (Dutta et al., 2014). As the role of
627 seedborne pathogens in causing yield losses receives relatively little attention, we hope that
628 the present study can stimulate novel research efforts in this sense to shed light on the many
629 obscure points still shrouding seed-pathogen interactions.

630

631 **Supplemental data**

632 Supplementary Data S1: Result tables of RNA-seq data

633 Supplementary Data S2: Result tables of sRNA-seq data

634 Supplementary Data S3: Result tables of BS-seq data

635 Supplementary Data S4: Primers used for qPCR experiments.

636

637 **Acknowledgements**

638 This work was supported by the French National Research Agency in the framework of the
639 SUCSEED project (ANR-20-PCPA-0009) and by the RFI "Objectif Végétal" supported by the
640 French Region Pays de la Loire, Angers Loire Métropole, and the European Regional
641 Development Fund. The authors wish to thank Daniel Sochard (Phenotic platform, SFR
642 Quasav) for crop management, Muriel Bahut (ANAN platform, SFR Quasav) for bacterial
643 RNA sequencing, Sébastien Carrère (LIPME, Toulouse) for the annotation of *Xcf* genome
644 sequences and Sylvain Gaillard for the public release of the Phaseolus Jbrowse.

645

646 **Author contributions**

647 AD, MBarret and JV designed the research. AD, MBarret and JV supervised the
648 experiments; AD, LPT, DL, NC, MBriand, MBarret, JV performed and analysed the
649 experiments. AD, LPT, NC, MBarret and JV wrote the manuscript and all co-authors
650 reviewed and edited the manuscript.

651

652 **Data availability**

653 The data that support the findings of this study have been deposited in NCBI Gene
654 Expression Omnibus and are accessible through GEO Super Series accession number
655 GSE227421 (<https://www.ncbi.nlm.nih.gov/geo/query/acc.cgi?acc=GSE227421>) or
656 individually through GEO accession numbers GSE227386 (bacterial RNA-seq,
657 <https://www.ncbi.nlm.nih.gov/geo/query/acc.cgi?acc=GSE227386>), GSE226918 (plant
658 RNAseq, <https://www.ncbi.nlm.nih.gov/geo/query/acc.cgi?acc=GSE226918>), GSE226919
659 (plant methylome, <https://www.ncbi.nlm.nih.gov/geo/query/acc.cgi?acc=GSE226919>) and
660 GSE226920 (sRNA-Seq, <https://www.ncbi.nlm.nih.gov/geo/query/acc.cgi?acc=GSE226920>).

661

662

663 **References**

- 664 **Ahmed I, Sarazin A, Bowler C, Colot V, Quesneville H** (2011) Genome-wide evidence for
665 local DNA methylation spreading from small RNA-targeted sequences in Arabidopsis.
666 *Nucleic Acids Res* **39**: 6919–6931
- 667 **Annacondia ML, Markovic D, Reig-Valiente JL, Scaltsoyiannes V, Pieterse CMJ,**
668 **Ninkovic V, Slotkin RK, Martinez G** (2021) Aphid feeding induces the relaxation of
669 epigenetic control and the associated regulation of the defense response in
670 Arabidopsis. *New Phytol* **230**: 1185–1200
- 671 **Bai Y, Meng Y, Huang D, Qi Y, Chen M** (2011) Origin and evolutionary analysis of the
672 plant-specific TIFY transcription factor family. *Genomics* **98**: 128–136
- 673 **Bethke G, Unthan T, Uhrig JF, Poschl Y, Gust AA, Scheel D, Lee J** (2009) Flg22
674 regulates the release of an ethylene response factor substrate from MAP kinase 6 in
675 Arabidopsis thaliana via ethylene signaling. *Proc Natl Acad Sci* **106**: 8067–8072
- 676 **Bhattarai KK, Atamian HS, Kaloshian I, Eulgem T** (2010) WRKY72-type transcription
677 factors contribute to basal immunity in tomato and Arabidopsis as well as gene-for-gene
678 resistance mediated by the tomato R gene Mi-1. *Plant J* **63**: 229–240
- 679 **Brewer PB, Howles PA, Dorian K, Griffith ME, Ishida T, Kaplan-Levy RN, Kilinc A,**
680 **Smyth DR** (2004) PETAL LOSS, a trihelix transcription factor gene, regulates perianth
681 architecture in the Arabidopsis flower. *Development* **131**: 4035–4045
- 682 **Briand M, Ruh M, Darrasse A, Jacques M-A, Chen NWG** (2021) Complete and

- 683 Circularized Genome Sequences of 17 *Xanthomonas* Strains Responsible for Common
684 Bacterial Blight of Bean. *Microbiol Resour Announc* **10**: e00371-21
- 685 **Büttner D** (2016) Behind the lines-actions of bacterial type III effector proteins in plant cells.
686 *FEMS Microbiol Rev* **40**: 894–937
- 687 **Catoni M, Tsang JM, Greco AP, Zabet NR** (2018) DMRcaller: a versatile R/Bioconductor
688 package for detection and visualization of differentially methylated regions in CpG and
689 non-CpG contexts. *Nucleic Acids Res* **46**: e114
- 690 **Cernay C, Ben-Ari T, Pelzer E, Meynard JM, Makowski D** (2015) Estimating variability in
691 grain legume yields across Europe and the Americas. *Sci Rep* **5**: 11171
- 692 **Chakraborty S, Nguyen B, Wasti SD, Xu G** (2019) Plant leucine-rich repeat receptor
693 kinase (LRR-RK): Structure, ligand perception, and activation mechanism. *Molecules*
694 **24**: 3081
- 695 **Chen NWG, Ruh M, Darrasse A, Foucher J, Briand M, Costa J, Studholme DJ, Jacques**
696 **MA** (2021a) Common bacterial blight of bean: a model of seed transmission and
697 pathological convergence. *Mol Plant Pathol* **22**: 1464–1480
- 698 **Chen S, Wu J, Zhang Y, Zhao Y, Xu W, Li Y, Xie J** (2021b) Genome-Wide Analysis of
699 Coding and Non-coding RNA Reveals a Conserved miR164–NAC–mRNA Regulatory
700 Pathway for Disease Defense in Populus. *Front Genet* **12**: 668940
- 701 **Chesneau G, Laroche B, Prévieux A, Marais C, Briand M, Marolleau B, Simonin M,**
702 **Barret M** (2022) Single Seed Microbiota: Assembly and Transmission from Parent
703 Plant to Seedling. *MBio* **13**: e0164822
- 704 **Dai X, Zhao PX** (2011) psRNATarget: a plant small RNA target analysis server. *Nucleic*
705 *Acids Res* **39**: W155-9
- 706 **Dai X, Zhuang Z, Zhao PX** (2018) psRNATarget: a plant small RNA target analysis server
707 (2017 release). *Nucleic Acids Res* **46**: W49–W54
- 708 **Darrasse A, Barret M, Cesbron S, Compant S, Jacques M-A** (2018) Niches and routes of
709 transmission of *Xanthomonas citri* pv. *fuscans* to bean seeds. *Plant Soil* **422**: 115–128
- 710 **Darrasse A, Bureau C, Samson R, Morris CE, Jacques M-A** (2007) Contamination of
711 bean seeds by *Xanthomonas axonopodis* pv. *phaseoli* associated with low bacterial
712 densities in the phyllosphere under field and greenhouse conditions. *Eur J Plant Pathol*
713 **119**: 203–215
- 714 **Darsonval A, Darrasse A, Durand K, Bureau C, Cesbron S, Jacques MA** (2009)
715 Adhesion and fitness in the bean phyllosphere and transmission to seed of
716 *xanthomonas fuscans* subsp. *Fuscans*. *Mol Plant-Microbe Interact* **22**: 747–757
- 717 **Darsonval A, Darrasse A, Meyer D, Demarty M, Durand K, Bureau C, Manceau C,**
718 **Jacques MA** (2008) The type III secretion system of *Xanthomonas fuscans* subsp.
719 *fuscans* is involved in the phyllosphere colonization process and in transmission to

- 720 seeds of susceptible beans. *Appl Environ Microbiol* **74**: 2669–2678
- 721 **Deleris A, Halter T, Navarro L** (2016) DNA Methylation and Demethylation in Plant
722 Immunity. *Annu Rev Phytopathol* **54**: 579–603
- 723 **Denancé N, Grimault V** (2022) Seed pathway for pest dissemination: The ISTA Reference
724 Pest List, a bibliographic resource in non-vegetable crops. *EPPO Bull* **52**: 434–445
- 725 **Dodds PN, Rathjen JP** (2010) Plant immunity: towards an integrated view of plant–
726 pathogen interactions. *Nat Rev Genet* **11**: 539–548
- 727 **Downen RH, Pelizzola M, Schmitz RJ, Lister R, Downen JM, Nery JR, Dixon JE, Ecker JR**
728 (2012) Widespread dynamic DNA methylation in response to biotic stress. *Proc Natl*
729 *Acad Sci U S A.* **109**: E2183-91
- 730 **Dutta B, Gitaitis R, Smith S, Langston D** (2014) Interactions of seedborne bacterial
731 pathogens with host and non-host plants in relation to seed infestation and seedling
732 transmission. *PLoS One* **9**: e99215
- 733 **Espinas NA, Saze H, Saijo Y** (2016) Epigenetic Control of Defense Signaling and Priming
734 in Plants. *Front Plant Sci* **7**: 1201
- 735 **Ferreira H, Pinto E, Vasconcelos MW** (2021) Legumes as a Cornerstone of the Transition
736 Toward More Sustainable Agri-Food Systems and Diets in Europe. *Front Sustain Food*
737 *Syst* **5**: 694121
- 738 **Figaj D, Ambroziak P, Przepiora T, Skorko-Glonek J** (2019) The Role of Proteases in the
739 Virulence of Plant Pathogenic Bacteria. *Int J Mol Sci* **20**: 672
- 740 **Fischer DS, Theis FJ, Yosef N** (2018) Impulse model-based differential expression analysis
741 of time course sequencing data. *Nucleic Acids Res* **46**: e119–e119
- 742 **Foucher J, Ruh M, Préveaux A, Carrère S, Pelletier S, Briand M, Serre R-F, Jacques M-
743 A, Chen NWG** (2020) Common bean resistance to *Xanthomonas* is associated with
744 upregulation of the salicylic acid pathway and downregulation of photosynthesis. *BMC*
745 *Genomics* **21**: 566
- 746 **Gitaitis R, Walcott R** (2007) The epidemiology and management of seedborne bacterial
747 diseases. *Annu Rev Phytopathol* **45**: 371–397
- 748 **Halter T, Wang J, Amesefe D, Lastrucci E, Charvin M, Singla Rastogi M, Navarro L**
749 (2021) The Arabidopsis active demethylase ROS1 cis-regulates defence genes by
750 erasing DNA methylation at promoter-regulatory regions. *Elife* **10**: e62994
- 751 **Hannan Parker A, Wilkinson SW, Ton J** (2022) Epigenetics: a catalyst of plant immunity
752 against pathogens. *New Phytol* **233**: 66–83
- 753 **Holt DB, Gupta V, Meyer D, Abel NB, Andersen SU, Stougaard J, Markmann K** (2015)
754 micro RNA 172 (miR172) signals epidermal infection and is expressed in cells primed
755 for bacterial invasion in *Lotus japonicus* roots and nodules. *New Phytol* **208**: 241–256
- 756 **Hou Y, Wang Y, Tang L, Tong X, Wang L, Liu L, Huang S, Zhang J** (2019) SAPK10-

- 757 Mediated Phosphorylation on WRKY72 Releases Its Suppression on Jasmonic Acid
758 Biosynthesis and Bacterial Blight Resistance. *iScience* **16**: 499–510
- 759 **Hu G, Lei Y, Liu J, Hao M, Zhang Z, Tang Y, Chen A, Wu J** (2020) The ghr-miR164 and
760 GhNAC100 modulate cotton plant resistance against *Verticillium dahlia*. *Plant Sci* **293**:
761 110438
- 762 **Johnson NR, Yeoh JM, Coruh C, Axtell MJ** (2016) Improved Placement of Multi-mapping
763 Small RNAs. *G3 (Bethesda)* **6**: 2103–2111
- 764 **Kim MJ, Jang I-C, Chua N-H** (2016) The Mediator Complex MED15 Subunit Mediates
765 Activation of Downstream Lipid-Related Genes by the WRINKLED1 Transcription
766 Factor. *Plant Physiol* **171**: 1951–1964
- 767 **Kozomara A, Birgaoanu M, Griffiths-Jones S** (2019) miRBase: from microRNA
768 sequences to function. *Nucleic Acids Res* **47**: D155–D162
- 769 **Krueger F, Andrews SR** (2011) Bismark: a flexible aligner and methylation caller for
770 Bisulfite-Seq applications. *Bioinformatics* **27**: 1571–1572
- 771 **Langmead B, Trapnell C, Pop M, Salzberg SL** (2009) Ultrafast and memory-efficient
772 alignment of short DNA sequences to the human genome. *Genome Biol* **10**: R25
- 773 **Li H, Handsaker B, Wysoker A, Fennell T, Ruan J, Homer N, Marth G, Abecasis G,
774 Durbin R** (2009) The Sequence Alignment/Map format and SAMtools. *Bioinformatics*
775 **25**: 2078–2079
- 776 **López Sánchez A, Stassen JHM, Furci L, Smith LM, Ton J** (2016) The role of DNA
777 (de)methylation in immune responsiveness of Arabidopsis. *Plant J* **88**: 361–374
- 778 **Love MI, Huber W, Anders S** (2014) Moderated estimation of fold change and dispersion
779 for RNA-seq data with DESeq2. *Genome Biol* **15**: 550
- 780 **Luo M, Luo M-Z, Buzas D, Finnegan J, Helliwell C, Dennis ES, Peacock WJ, Chaudhury
781 A** (2008) UBIQUITIN-SPECIFIC PROTEASE 26 Is Required for Seed Development and
782 the Repression of PHERES1 in Arabidopsis. *Genetics* **180**: 229–236
- 783 **Martinez-Medina A, Flors V, Heil M, Mauch-Mani B, Pieterse CMJ, Pozo MJ, Ton J, van
784 Dam NM, Conrath U** (2016) Recognizing Plant Defense Priming. *Trends Plant Sci* **21**:
785 818–822
- 786 **Martins D, Araújo S de S, Rubiales D, Vaz Patto MC** (2020) Legume Crops and Biotrophic
787 Pathogen Interactions: A Continuous Cross-Talk of a Multilayered Array of Defense
788 Mechanisms. *Plants (Basel)* **9**: 1460
- 789 **Maude RB** (1996) Seedborne Diseases and Their Control: Principles and Practice. CAB
790 International
- 791 **Maury Y, Duby C, Bossenec J-M, Boudazin G** (1985) Group analysis using ELISA: \square :
792 determination of the level of transmission of Soybean Mosaic Virus in soybean seed.
793 *Agronomie* **5**: 405–415

- 794 **Mozgová I, Wildhaber T, Liu Q, Abou-Mansour E, L'Haridon F, Métraux JP, Gruissem**
795 **W, Hofius D, Hennig L** (2015) Chromatin assembly factor CAF-1 represses priming of
796 plant defence response genes. *Nat Plants* **1**: 15127
- 797 **Myers SS, Zanobetti A, Kloog I, Huybers P, Leakey ADB, Bloom AJ, Carlisle E,**
798 **Dietterich LH, Fitzgerald G, Hasegawa T, et al** (2014) Increasing CO₂ threatens
799 human nutrition. *Nature* **510**: 139–142
- 800 **Narsai R, Gouil Q, Secco D, Srivastava A, Karpievitch Y V, Liew LC, Lister R, Lewsey**
801 **MG, Whelan J** (2017) Extensive transcriptomic and epigenomic remodelling occurs
802 during *Arabidopsis thaliana* germination. *Genome Biol* **18**: 172
- 803 **Noman A, Liu Z, Aqeel M, Zainab M, Khan MI, Hussain A, Ashraf MF, Li X, Weng Y, He**
804 **S** (2017) Basic leucine zipper domain transcription factors: the vanguards in plant
805 immunity. *Biotechnol Lett* **39**: 1779–1791
- 806 **Ortega-Cuadros M, De Souza TL, Berruyer R, Aligon S, Pelletier S, Renou JP, Arias T,**
807 **Campion C, Guillemette T, Verdier J, et al** (2022) Seed Transmission of Pathogens:
808 Non-Canonical Immune Response in *Arabidopsis* Germinating Seeds Compared to
809 Early Seedlings against the Necrotrophic Fungus *Alternaria brassicicola*. *Plants (Basel)*
810 **11**: 1708
- 811 **Patro R, Duggal G, Love MI, Irizarry RA, Kingsford C** (2017) Salmon provides fast and
812 bias-aware quantification of transcript expression. *Nat Methods* **14**: 417–419
- 813 **Pruitt RN, Locci F, Wanke F, Zhang L, Saile SC, Joe A, Karelina D, Hua C, Fröhlich K,**
814 **Wan WL, et al** (2021) The EDS1–PAD4–ADR1 node mediates *Arabidopsis* pattern-
815 triggered immunity. *Nature* **598**: 495–499
- 816 **Schwacke R, Ponce-Soto GY, Krause K, Bolger AM, Arsova B, Hallab A, Gruden K,**
817 **Stitt M, Bolger ME, Usadel B** (2019) MapMan4: A Refined Protein Classification and
818 Annotation Framework Applicable to Multi-Omics Data Analysis. *Mol Plant* **12**: 879–892
- 819 **Shivaprasad P V, Chen H-M, Patel K, Bond DM, Santos BACM, Baulcombe DC** (2012) A
820 MicroRNA Superfamily Regulates Nucleotide Binding Site–Leucine-Rich Repeats and
821 Other mRNAs. *Plant Cell* **24**: 859–874
- 822 **Slaughter A, Daniel X, Flors V, Luna E, Hohn B, Mauch-Mani B** (2012) Descendants of
823 Primed *Arabidopsis* Plants Exhibit Resistance to Biotic Stress. *Plant Physiol* **158**: 835–
824 843
- 825 **Soto-Suárez M, Baldrich P, Weigel D, Rubio-Somoza I, San Segundo B** (2017) The
826 *Arabidopsis* miR396 mediates pathogen-associated molecular pattern-triggered
827 immune responses against fungal pathogens. *Sci Rep* **7**: 44898
- 828 **Stagnari F, Maggio A, Galieni A, Pisante M** (2017) Multiple benefits of legumes for
829 agriculture sustainability: an overview. *Chem Biol Technol Agric* **4**: 2
- 830 **Teper D, Pandey SS, Wang N** (2021) The HrpG/HrpX Regulon of Xanthomonads-An Insight

- 831 to the Complexity of Regulation of Virulence Traits in Phytopathogenic Bacteria.
832 *Microorganisms* **9**: 187
- 833 **Terrasson E, Darrasse A, Righetti K, Buitink J, Lalanne D, Ly Vu B, Pelletier S,**
834 **Bolingue W, Jacques MA, Leprince O** (2015) Identification of a molecular dialogue
835 between developing seeds of *Medicago truncatula* and seedborne xanthomonads. *J*
836 *Exp Bot* **66**: 3737–3752
- 837 **Tintor N, Ross A, Kanehara K, Yamada K, Fan L, Kemmerling B, Nürnberger T, Tsuda**
838 **K, Saijo Y** (2013) Layered pattern receptor signaling via ethylene and endogenous
839 elicitor peptides during *Arabidopsis* immunity to bacterial infection. *Proc Natl Acad Sci U*
840 *S A* **110**: 6211–6216
- 841 **Varet H, Brillet-Guéguen L, Coppée J-Y, Dillies M-A** (2016) SARTools: A DESeq2- and
842 EdgeR-Based R Pipeline for Comprehensive Differential Analysis of RNA-Seq Data.
843 *PLoS One* **11**: e0157022
- 844 **Wirthmueller L, Maqbool A, Banfield MJ** (2013) On the front line: structural insights into
845 plant-pathogen interactions. *Nat Rev Microbiol* **11**: 761–776
- 846 **Yu C, Song L, Song J, Ouyang B, Guo L, Shang L, Wang T, Li H, Zhang J, Ye Z** (2018)
847 ShCIGT, a Trihelix family gene, mediates cold and drought tolerance by interacting with
848 SnRK1 in tomato. *Plant Sci* **270**: 140–149
- 849 **Yu G, Wang L-G, Han Y, He Q-Y** (2012) clusterProfiler: an R package for comparing
850 biological themes among gene clusters. *OMICS* **16**: 284–287

851

852

853

854 **Legends**

855 **Figure 1. Transmission of *Xcf* to bean seeds.** (A) Seed water content (B) Seed dry weight
856 (gram) and (C) *Xcf* population size (\log_{10} CFU per gram of seed) at the different sampling
857 stages (24DAP, 35DAP and 42DAP). Differences between the sampling stage and the
858 treatment (H_2O - or *Xcf*-inoculated) were assessed by Kruskal-Wallis test followed by post-
859 hoc Dunn's test. The percentages of observed contaminated seeds at different seed
860 developmental stages are indicated (expressed as averages with SD between brackets). P-
861 values are indicated as * <5%, ** <1% and *** <0.1%.

862

863 **Figure 2. Dual transcriptomic analysis of the *Xcf*-*P. vulgaris* seed interaction.** (A) & (C)
864 Histograms summarizing the number of differentially expressed genes (DEGs) detected
865 comparing datasets from different seed development stages from *Xcf* samples (A) and
866 DEGs from different development stages from *P. vulgaris* samples (C). The number of DEGs

867 is indicated on the bars. **(B) & (D)** Dot plots showing category enrichment results obtained
868 through gene ontology analysis of DEGs from *Xcf* **(B)** and *P. vulgaris* **(D)**. Gene ontology
869 analysis was performed with the ClusterProfiler package for R.

870 **Figure 3. Summary of methylome analysis data generated by comparing *Xcf*-colonized**
871 **and uncolonized seeds at 42 DAP.** **(A)** Pie chart illustrating the repartition of differentially
872 methylated regions (DMRs) following *Xcf* colonization on *P. vulgaris* genome at 42 DAP. **(B)**
873 Venn diagram illustrating the overlap between gene sequences containing DMRs at 42 DAP
874 and differentially expressed genes (DEGs) during germination (see details in text).

875 **Figure 4. Schematic model of the *Xcf*-bean seed dialogue.** Left panel: at early seed
876 development stages (24 DAP), *Xcf* is recognized by the host. Despite the bacterial
877 recognition, defense transduction pathways based on MAP kinases cascades (MAPKs) and
878 transcription factors (TFs) activation are suppressed in seeds, thus failing to induce a
879 defense reaction. Red dotted lines with flat end indicate hypothetical inhibition. Middle Panel:
880 at 35 DAP, both the bacterial pathogen and the host plant are still transcriptionally active.
881 Bacterial populations continue to grow, but the T3SS is no longer active, suggesting that the
882 bacteria lowered its weapons, keeping the seed alive and healthy. Right panel: at seed
883 maturation (42 DAP), the dialogue between *Xcf* and seed is much less detectable in
884 comparison to earlier stages but epigenetic mechanisms such as DNA methylation could be
885 active, which was observed at seed maturity by the changes in the methylation status of
886 genes identified as involved in both defense and germination processes. This change in
887 DNA methylation could prime genes involved in defense/germination, ultimately preparing
888 the host for the post-germination battle with the virulent *Xcf* (see text for more details).

889

890

891

892

893

894

895

896

897

898

899

900

901

902

903

904

905

906

907

908

909

910 Tables

911 **Table 1. Summary of differentially accumulated small RNAs (up- or down-regulated)**
 912 **detected at 24 and 42 DAP in *Xcf*-colonized *P. vulgaris* seeds with their putative target**
 913 **genes according to psRNAtarget.**

Seed developmental stages	DEseq2			psRNAtarget combined with corresponding significant expression changes from RNAseq data putative targets using psRNAtarget (= miRNA potential target genes)
	Up- or down-regulation in <i>Xcf</i> -colonized seeds	mature miR	variants	
24DAP	Up	miR162	a,b	Phvul.007G067800 (HSF), Phvul.008G055500 (TG D3), Phvul.006G176000 (trihelix DNA-binding), Phvul.008G114700 (Rab-GDF)
	Up	miR172	a,c,d,e,f,g,h,i,l	Phvul.009G014600 (cardiolipin deacylase), Phvul.001G212400 (RING-domain E3 ligase), Phvul.005G068800 (Probable E3 ubiquitin-protein ligase), Phvul.003G053000 (glycosyltransferase)
	Up	miR396	a,b,c,d,e,i	Phvul.009G246000 (SNF4-like), Phvul.001G229200 (pepsin-type protease), Phvul.002G026300 (integrin-like protein), Phvul.003G154800 (HSP70)
	Up	miR482	3p, b-3p, d-3p	Phvul.011G149100 Transducin/WD40 repeat-like), Phvul.008G055500 (ATPase component TG D3 of TGD), Phvul.003G295800 (ATG 2-like), Phvul.011G082700 (P-loop NTPase), Phvul.010G141400 (DOF1-like TF), Phvul.002G261500 (RNA polymerase regulatory protein)
	Up	miR6478	-	Phvul.003G155500 (component SR-alpha of SRP)
	Up	miR8175	-	Phvul.002G059000 (Phospholipase A1), Phvul.002G274500 (PAD4-like), Phvul.010G082300 (UDP-D-glucuronic acid 4-epimerase), Phvul.005G035400 (mRNA-splicing factor 18), Phvul.001G240600 (CaLB domain)
	Down	let7	a,c,d,f	Phvul.001G022700 (REMORIN-LIKE), Phvul.003G119100 (calcium-dependent lipid-binding), Phvul.011G061600 (PTAC16-like), Phvul.003G035400 (XYL1-like), Phvul.004G121666 (subunit of CF1 of ATP synthase), Phvul.008G163350 (cohesin cofactor (PD55)), Phvul.011G050300 (protein kinase (PIKK) TOR-like), Phvul.003G050600 (catalytic protein (CER2)), Phvul.007G069900, Phvul.011G001200 (SAC1-like), Phvul.002G185150 (sodium:proton antiporter (SOS1))
	Down	miR21	a	Phvul.010G157900 (MED15-like), Phvul.007G191600 (CHR8-like)
	Down	miR2111	a,b,c,d,e,f,g,h,l,j,k,m,n,o	Phvul.001G269300 (MED13-like), Phvul.001G179300 (PGP1-like), Phvul.010G125200 (NOC1/SWA2-like), Phvul.007G168500 (Solute transport channels)
Down	miR482	5p	Phvul.004G170000 (STT3-like), Phvul.010G125200 (NOC1/SWA2-like), Phvul.007G244066, Phvul.002G189700 (UPL1-like)	
42DAP	Up	miR31	-	-
	Down	miR451	a	Phvul.009G100000 (UBP26-like)
	Down	miR164	a,b,c,d,e,f,g,h,l,j,k	-

914

915

916

917

918

919

920

921

922

923

924

925

926

927

928

929

930

931

932

933 **Table 2. List of differentially methylated regions located in defense-associated genes**
934 **in of *P. vulgaris* seeds following *Xcf* colonization at 42 DAP. DMRs were located in**
935 **promoter or gene sequences, but also in transposable elements located within 5kb of**
936 **genic regions.** The *P. vulgaris* annotation column was filled according to the *P. vulgaris*
937 genome (v2.1). The location indicates whether the region is localized in a coding region
938 (gene) or in the promoter (1kbprom) or in TE within 5kb of genic regions (within 5kb). The
939 putative ortholog was assigned as best hit based on sequence similarity in the *A. thaliana*
940 genome (v.11). The “gain or loss” column shows whether the differentially methylated region
941 associated with the corresponding *P. vulgaris* gene is hypo- (loss) or hypermethylated (gain)
942 in response to *Xcf* colonization at 42 DAP. FC, fold change of methylation between *Xcf*-
943 versus H₂O-treated seeds. FC ratios are not indicated for DMRs within 5kb of genic regions
944 because they correspond to multiple DMRs.

945

<i>P. vulgaris</i> locus ID	Location	<i>P. vulgaris</i> annotation	<i>A. thaliana</i> putative ortholog	<i>A. thaliana</i> symbol	<i>A. thaliana</i> annotation	Methylation FC (Xcf vs H2O)	Gain or loss of methylation in Xcf-treated seeds
Phvul.001G233000	gene	protein kinase [SD-1]	AT3G16030	CE5J01	lectin protein kinase family protein	0.52	loss
Phvul.002G125500	within 5kb	not annotated	AT5G08315		Defensin-like [DEF1] family protein		loss
Phvul.002G130300	within 5kb	not annotated	AT3G14470		NB-ARC domain-containing disease resistance protein		gain
Phvul.002G130400	within 5kb	not annotated	AT3G14470		NB-ARC domain-containing disease resistance protein		gain
Phvul.003G021700	1 kb Prom	transferase transferring phosphorus-containing group	AT3G07040		Protein kinase superfamily protein	0.51	loss
Phvul.003G040300	1 kb Prom	6-deoxocastasterone 6-oxidase	AT3G03180	BR6OX2	brassinosteroid-6-oxidase 2	2.98	gain
Phvul.003G056900	within 5kb	systemic acquired resistance [SAR] regulator protein [SN1]	AT4G18470	SN1	negative regulator of systemic acquired resistance [SN1]		loss
Phvul.003G068700	gene	transcription factor [WRKY]	AT5G15130	WRKY72	WRKY DNA-binding protein 72	4.50	gain
Phvul.003G068700	within 5kb	transcription factor [WRKY]	AT5G15130	WRKY72	WRKY DNA-binding protein 72		gain
Phvul.003G175700	gene	DRB4-DRB7.1 regulator complex component DRB7	AT5G20320	DCL4	dicer-like 4	0.37	loss
Phvul.004G076200	within 5kb	not annotated	AT3G14470		NB-ARC domain-containing disease resistance protein		loss
Phvul.004G105600	within 5kb	not annotated	AT2G34930		disease resistance family protein / LRR family protein		loss
Phvul.005G162000	1 kb Prom	transferase transferring phosphorus-containing group	AT4G29990		Leucine-rich repeat transmembrane protein kinase protein	2.56	gain
Phvul.005G162000	within 5kb	transferase transferring phosphorus-containing group	AT4G29990		Leucine-rich repeat transmembrane protein kinase protein		gain
Phvul.005G162100	within 5kb	transferase transferring phosphorus-containing group	AT1G51800		Leucine-rich repeat protein kinase family protein		gain
Phvul.005G163000	gene	transferase transferring phosphorus-containing group	AT4G29990		Leucine-rich repeat transmembrane protein kinase protein	0.38	loss
Phvul.005G163000	within 5kb	transferase transferring phosphorus-containing group	AT4G29990		Leucine-rich repeat transmembrane protein kinase protein		loss
Phvul.006G006800	gene	TKL protein kinase superfamily protein kinase [DUF261]	AT4G05200	CRK25	cysteine-rich RLK/RECEPTOR-like protein kinase 25	0.18	loss
Phvul.006G033200	gene	not annotated	AT5G38280	PR5K	PR5-like receptor kinase	0.52	loss
Phvul.007G187700	1 kb Prom	not annotated	AT3G04720	PR4	pathogenesis-related 4	0.37	loss
Phvul.007G241200	gene	transcription factor [MYB-related]	AT5G47390		myb-like transcription factor family protein	3.25	gain
Phvul.007G241200	within 5kb	transcription factor [MYB-related]	AT5G47390		myb-like transcription factor family protein		gain
Phvul.007G241300	within 5kb	Ser/Thr protein kinase	AT1G50240	FU	Protein kinase family protein with ARM repeat domain		gain
Phvul.008G164500	within 5kb	transferase transferring phosphorus-containing group	AT3G21340		Leucine-rich repeat protein kinase family protein		loss
Phvul.008G164600	gene	not annotated	AT1G05700		Leucine-rich repeat transmembrane protein kinase protein	0.45	loss
Phvul.008G164600	within 5kb	not annotated	AT1G05700		Leucine-rich repeat transmembrane protein kinase protein		loss
Phvul.008G228714	gene	S8-class protease/subtilisin family protease [SBT4]	AT3G46850		Subtilase family protein	4.29	gain
Phvul.008G229400	gene	S8-class protease/subtilisin family protease [SBT4]	AT5G59100		Subtilisin-like serine endopeptidase family protein	0.48	loss
Phvul.010G026400	1 kb Prom	effector receptor [NLR]	AT5G36930		Disease resistance protein [TIR-NBS-LRR class] family	0.35	loss
Phvul.010G026400	within 5kb	effector receptor [NLR]	AT5G36930		Disease resistance protein [TIR-NBS-LRR class] family		loss
Phvul.010G027900	within 5kb	effector receptor [NLR]	AT5G36930		Disease resistance protein [TIR-NBS-LRR class] family		loss
Phvul.010G028000	within 5kb	effector receptor [NLR]	AT5G36930		Disease resistance protein [TIR-NBS-LRR class] family		loss
Phvul.010G062500	within 5kb	WRKY33-dependent plant immunity transcription factor	AT2G38470	WRKY33	WRKY DNA-binding protein 33		loss
Phvul.011G064700	gene	U-Box E3 ligase activator E3 ubiquitin ligase [PUB]	AT3G46510	PUB13	plant U-box 13	4.06	gain
Phvul.011G108300	gene	transferase transferring phosphorus-containing group	AT1G29730		Leucine-rich repeat transmembrane protein kinase	2.32	gain
Phvul.011G176300	gene	transferase transferring carbon group	AT3G12480	BSMT1	S-adenosyl-L-methionine-dependent methyltransferase family protein	2.56	gain

946

947

948

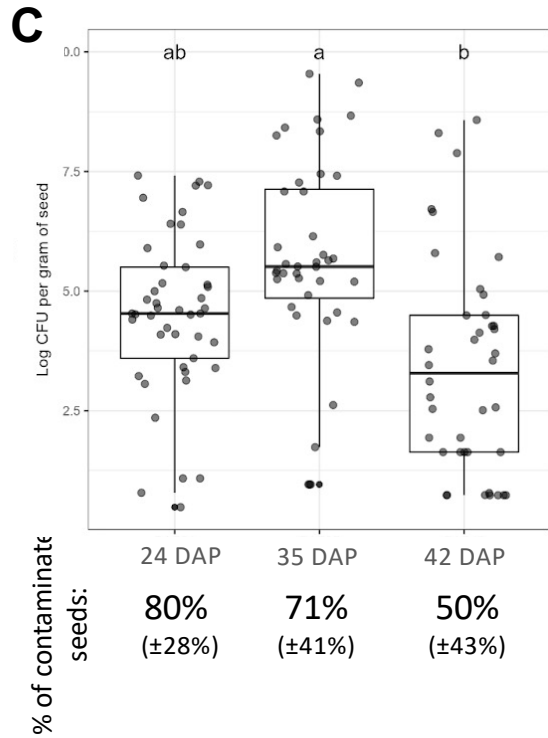
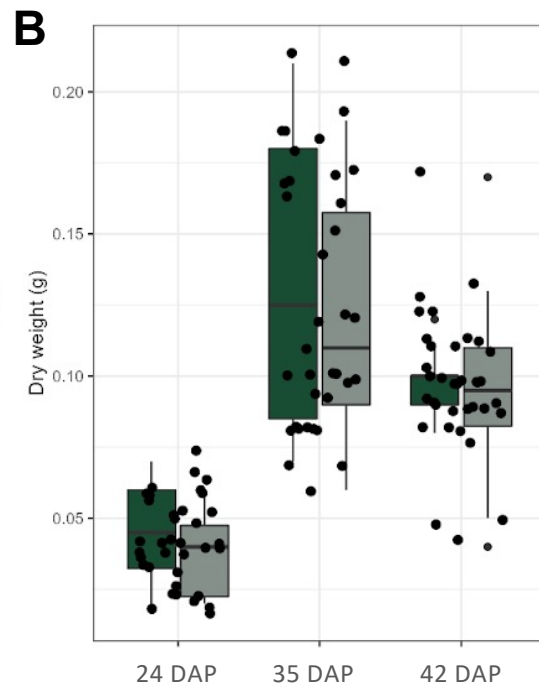
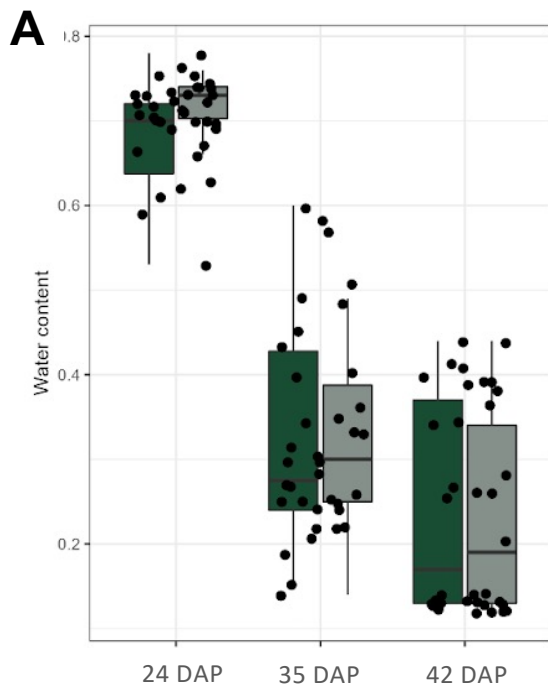


Figure 1. Transmission of *Xcf* to bean seeds. (A) Seed water content (B) Seed dry weight (gram) and (C) *Xcf* population size (\log_{10} CFU per gram of seed) at the different sampling stages (24DAP, 35DAP and 42DAP). Differences between the sampling stage and the treatment (H_2O - or *Xcf*-inoculated) were assessed by Kruskal-Wallis test followed by post-hoc Dunn's test. The percentages of observed contaminated seeds at different seed developmental stages are indicated (expressed as averages with SD between brackets). P-values are indicated as * <5%, ** <1% and *** <0.1%.

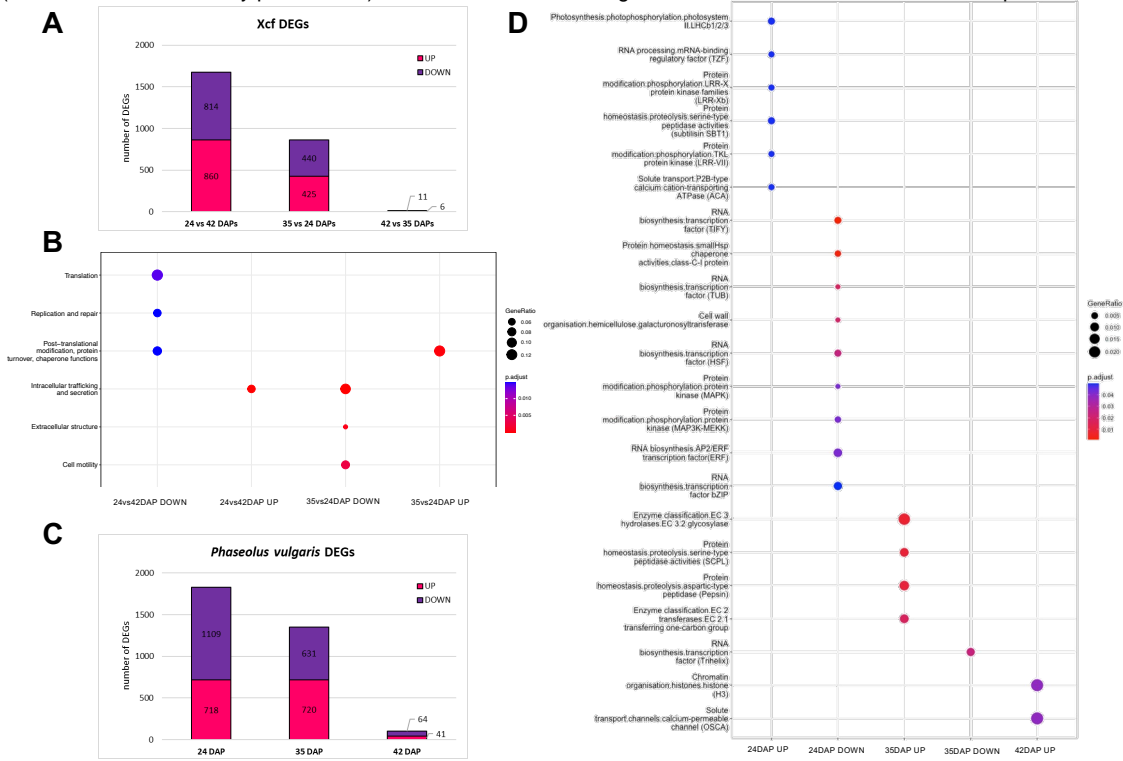


Figure 2. Dual transcriptomic analysis of the *Xcf-P. vulgaris* seed interaction.

(A)(C) Histograms summarizing the number of differentially expressed genes (DEGs) detected comparing datasets from different seed development stages from *Xcf* samples (A) and DEGs from different development stages from *P. vulgaris* samples (C). The number of DEGs is indicated on the bars. (B) (D) Dot plots showing category enrichment results obtained through gene ontology analysis of DEGs from *Xcf* (B) and *P. vulgaris* (D). Gene ontology analysis was performed with the Clusterprofiler package for R.

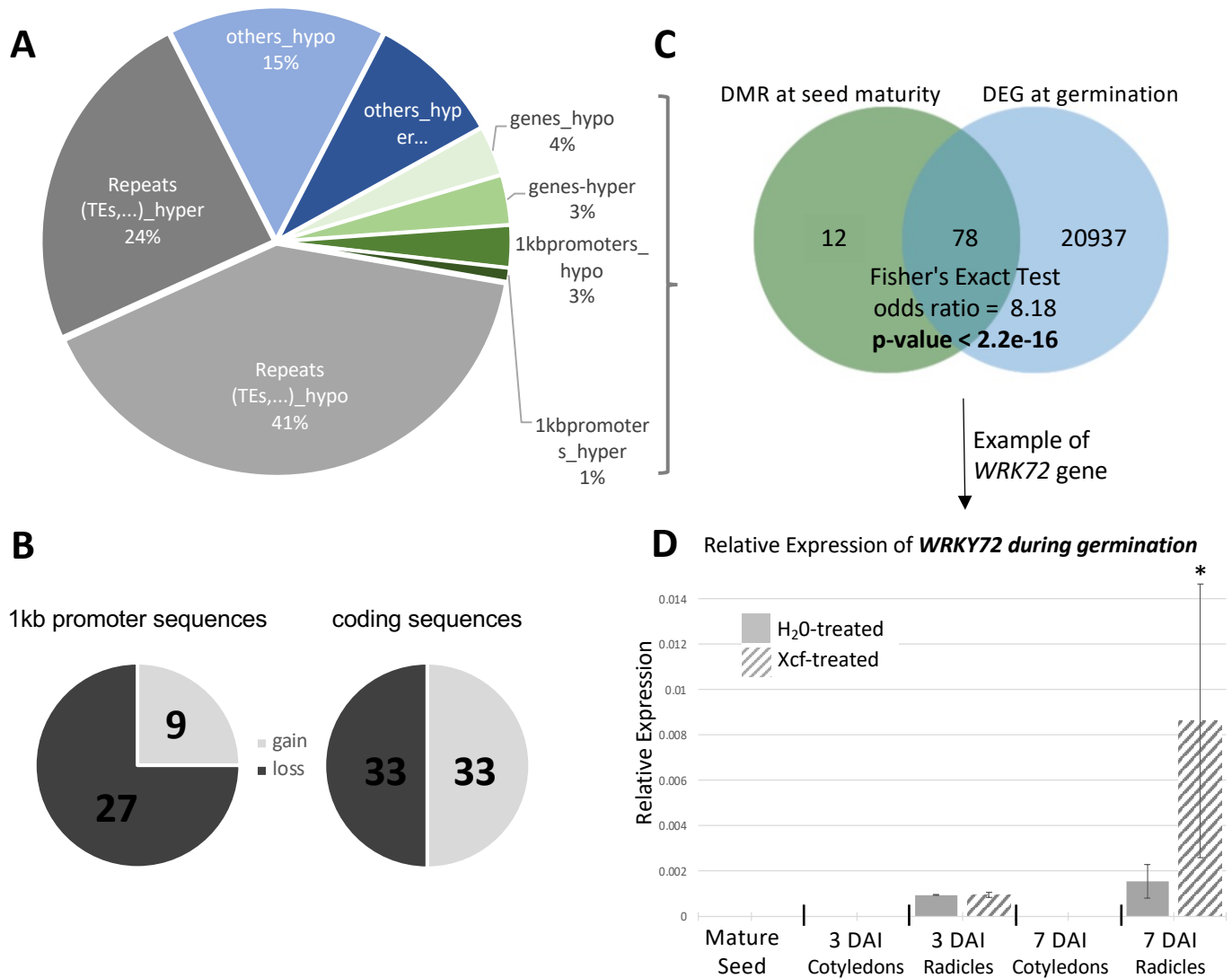


Figure 3. Summary of methylome analysis data generated by comparing *Xcf*-colonized and uncolonized seeds at 42 DAP. (A) Pie chart illustrating the repartition of differentially methylated regions (DMRs) following *Xcf* colonization on *P. vulgaris* genome at 42 DAP. (B) Pie charts illustrating the number of hypo-(loss) and hyper-(gain) methylated DMRs located in annotated genes (1kb promoter or coding sequences). (C) Venn diagram illustrating the overlap between gene sequences containing DMRs at 42 DAP and differentially expressed genes (DEGs) during germination (see details in text). (D) Relative expression of *WRKY72* during germination (at 3 and 7 Days after imbibition, DAI) in H₂O- and *Xcf*-treated seeds.

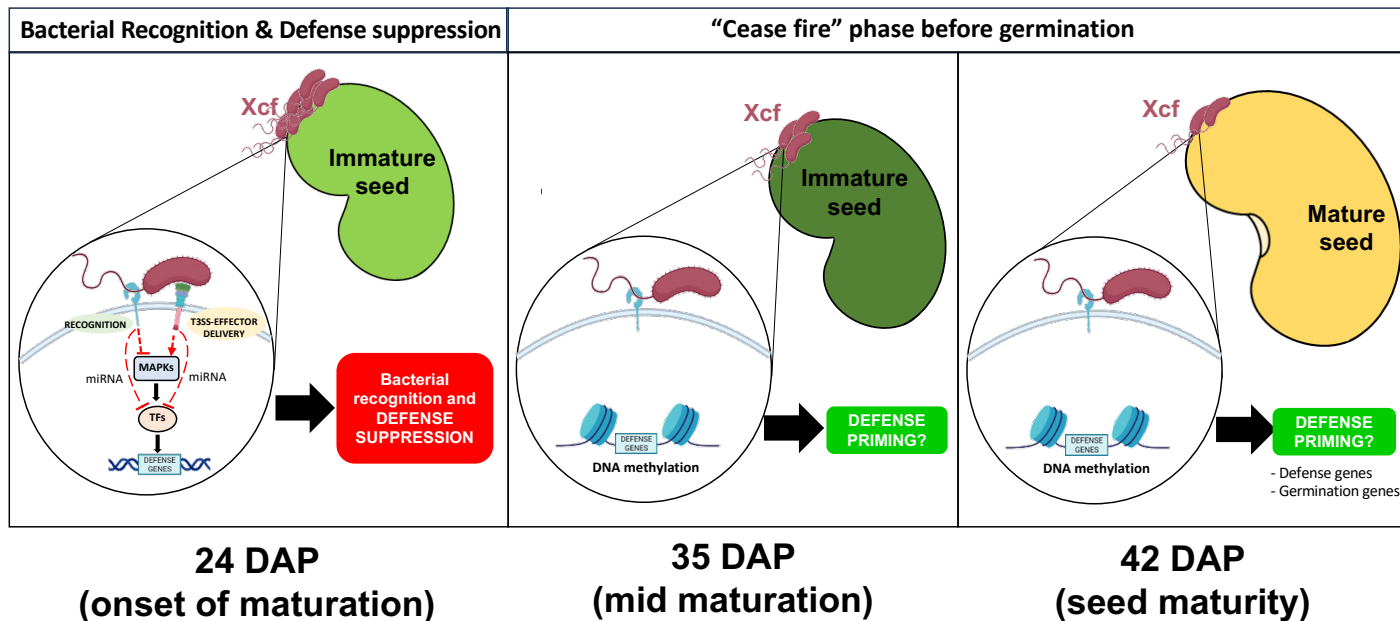


Figure 4. Schematic model of the *Xcf*-bean seed dialogue. Left panel: at early seed development stages (24 DAP), *Xcf* is recognized by the host. Despite the bacterial recognition, defense transduction pathways based on MAP kinases cascades (MAPKs) and transcription factors (TFs) activation are suppressed in seeds, thus failing to induce a defense reaction. Red dotted lines with flat end indicate hypothetical inhibition. Middle Panel: at 35 DAP, both the bacterial pathogen and the host plant are still transcriptionally active. Bacterial populations continue to grow, but the T3SS is no longer active, suggesting that the bacteria lowered its weapons, keeping the seed alive and healthy. Right panel: at seed maturation (42 DAP), the dialogue between *Xcf* and seed is much less detectable in comparison to earlier stages but epigenetic mechanisms such as DNA methylation could be active, which was observed at seed maturity by the changes in the methylation status of genes identified as involved in both defense and germination processes. This change in DNA methylation could prime genes involved in defense/germination, ultimately preparing the host for the post-germination battle with the virulent *Xcf* (see text for more details).